Lateral pressure on piles due to horizontal soil movement - 1g model tests on single piles and pile rows

J. Bauer, H.-G. Kempfert & O. Reul
University of Kassel, Germany

ABSTRACT: In soft soil layers vertical piles are frequently loaded laterally by horizontal soil movements caused by eccentric loading or unloading of the ground surface around the piles. In many cases, the lateral pressure acting on piles due to horizontal soil movements is calculated with empirically or analytically based approaches, respectively. In the scope of this paper the results of 1g model tests on single piles and pile rows in Kaolin clay are presented. During the model tests the soil movements were analyzed with the PIV-Method. The model tests investigate the influence of the roughness of the pile-soil-interface, the pile shape and the displacement rate of the soft soil flowing around the pile on the lateral pressure acting on the piles.

1 INTRODUCTION

According to de Beer (1977) horizontally loaded piles can be classified into "active piles" and "passive piles". "Active piles" are subjected to horizontal loads at the pile head caused by the superstructure.

"Passive piles" are frequently found in soft soil layers where eccentric loading or unloading of the ground surface around piles causes horizontal soil movements resulting in a lateral pressure on adjacent piles. Typical examples are embankments behind piled bridge abutments or piles close to excavations (Figure 1).

In many cases, the lateral pressure acting on piles due to horizontal soil movements is calculated with empirical formulae or analytically based on plasticity or earth pressure theory, respectively.

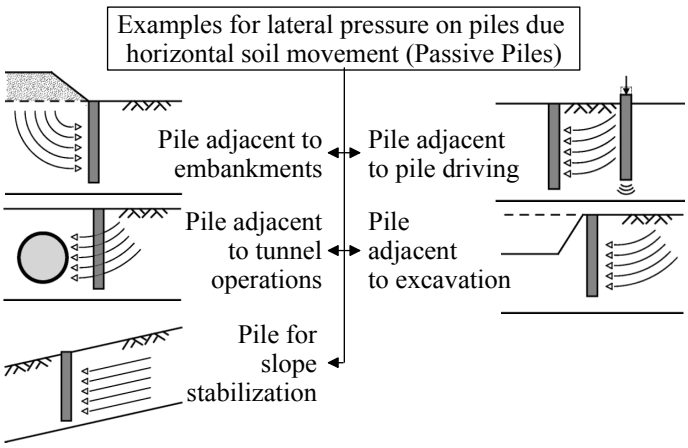

Figure 1. Lateral pressure on piles due to horizontal soil movement (after Chen 2004).

However, most of these calculation methods do not consider possible influences on the resulting pile loads such as the roughness of the pile-soil-interface, the pile shape or the visco-plastic material behaviour of soft soils.

In the scope of this paper the results of 1g model tests in Kaolin clay on piles subjected to lateral pressure, which were carried out to overcome some of these limitations and to improve the available design approaches, are presented.

2 LATERAL PRESSURE ON PILES DUE TO HORIZONTAL SOIL MOVEMENT

2.1 *Model tests*

An overview of selected 1g- and centrifuge model tests carried out on laterally loaded single piles and pile groups in horizontally moving clayey soils is given in Table 1. Varying boundary conditions such as the constraints at the pile head and the pile spacing were investigated.

Typical techniques for the activation of lateral pressure on model piles are depicted in Figure 2 with the test carried out load- or displacement-controlled, respectively.

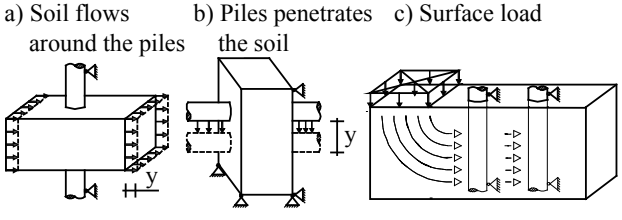

Figure 2. Activation of lateral pressure in model tests.

Table 1. Model tests in clayey soils.

Reference	Activation of lateral pressure (Figure 2)	Soil layers (from top to down)
1g model tests		
Wenz (1963)	a); SP, PG	Clay
Matsui et al. (1982)	a); PG	Clay
Pan et al. (2000, 2002)	a); SP, PG	Kaolin clay
Knappett et al. (2010)	a); SP	Kaolin clay
Centrifuge model tests		
Springman (1989)	c); PG	Sand-Clay-Sand
Stewart (1992)	c); PG	Clay-Sand
Bransby (1995)	c); PG	Sand-Clay-Sand
Ong et al. (2003)	c); SP, PG	Clay-Sand
Jeong et al. (2004)	c); PG	Sand-Clay-Sand

SP = Single Pile; PG = Pile Groups

2.2 *Design methods*

According to Stewart et al. (1994) the broad groupings for existing design methods are
- empirical methods,
- pressure-based methods,
- displacement-based methods,
- finite element analyses.

Previous studies (e. g. Gudehus & Leinenkugel 1978; Randolph & Houlsby 1984) indicate that the lateral pressure on piles depends on various parameters such as
- pile roughness,
- pile shape,
- pile flexibility,
- velocity of the soil flowing around the pile

However, in design practice frequently the following simplified expression is applied

$$P_u = \chi \cdot s_u \cdot d_p \quad \text{or} \quad P_u = \chi \cdot s_u \cdot a_p \tag{1}$$

where P_u = lateral pressure on the pile; χ = empirically or theoretically derived coefficient; s_u = undrained shear strength; d_p = pile diameter; a_p = edge length of the pile.

In German design practice, additionally the lateral pressure P_e is estimated based on earth pressure theory. The smaller value of the two parameters P_e and P_u is then applied for the pile design (DGGT AK 2.1 2012). Table 2 gives an overview of design methods applying Equation 1.

3 1G MODEL TESTS ON SINGLE PILES AND PILE ROWS

3.1 *Test set-up*

For the 1g model tests summarized in Table 3 the approach sketched in Figure 2a was adopted, i. e. the soil (Kaolin clay) flows around fixed single piles or pile rows, respectively. Figure 3 shows the test set up. The soil is located in a box on a cart which is pulled displacement-controlled by means of a hydraulic press.

Table 2. Design method for the lateral pressure P_u.

Reference	Derivation	P_u
DGGT AK 2.1 (2012)	theoretical	$7.0 \cdot s_u \cdot d_P$
Brinch Hansen &	theoretical	$7.5 \cdot s_u \cdot a_P$
Lundgren (1960)		$6.4 \cdot s_u \cdot d_P$
Schenk &	theoretical	$3.4 \cdot s_u \cdot a_P$
Smoltczyk (1966)		$2.6 \cdot s_u \cdot d_P$
Wenz (1963)	1g model tests	$\approx 8.3 \cdot s_u \cdot a_P$
Wenz (1972)	theoretical	$11.4 \cdot s_u \cdot a_P$
Gudehus & Leinen-	theoretical	
kugel (1978)		$4.5 \cdot s_u \cdot d_P$
Randolph &	theoretical*	$9.14 \cdot s_u \cdot d_P$
Houlsby (1984)		$11.94 \cdot s_u \cdot d_P$
Chen (1994)	FE-Analysis	$11.4 \cdot s_u \cdot a_P$
Bransby (1995)	FE-Analysis	$11.75 \cdot s_u \cdot d_P$
Pan et al. (2000)	1g model tests	$\approx 10.6 \cdot s_u \cdot a_P$
Knappett et al. (2010)	1g model tests	$8.33 \cdot s_u \cdot a_P$
		$8.62 \cdot s_u \cdot d_P$

* Results for perfectly smooth and perfectly rough piles

The wheels of the cart are guided in steel channel sections. The ground area of the 200 mm deep box was variable within maximum dimensions of 840 mm × 1120 mm. Based on the PIV observations, the zone of deforming soil around the pile did not extend to the container boundaries. A spring prevented cart movements during initial adjustments of the press.

During the tests, each model pile was fixed by means of two guyings aligned with the direction of the soil movement. The guyings were connected with the back of the pile near the pile head and the pile base, respectively. A guying comprises a steel cable connected to a load cell which allowed for the measurement of forces acting on the pile due to the soil movement independently from the hydraulic press pulling the cart. Additionally, the pile base was equipped with a ball bearing to prevent excessive friction and was located in a guide rail. During the soil placement in the box, the piles were temporarily supported by means of two guyings between the pile head and the box walls.

The 200 mm long model piles were fabricated from aluminium profiles with circular or square cross sections, respectively. Diameters d_p and edge length a_p ranged between 20 mm to 40 mm. The plain surfaces of the aluminium profiles are considered as "smooth" in the scope of this work. For the investigation of "rough" piles, sandpaper was glued on the aluminium profiles.

The resistance of the cart comprising inertia forces, friction and spring resistance was measured after every test when the box filled with soil but with the piles already extracted was moved.

For the investigation of pile rows, two or three piles, respectively, were lined up perpendicular to the direction of the soil movement (Figure 4). Guy cables between pile heads prevented relative displacements among the piles.

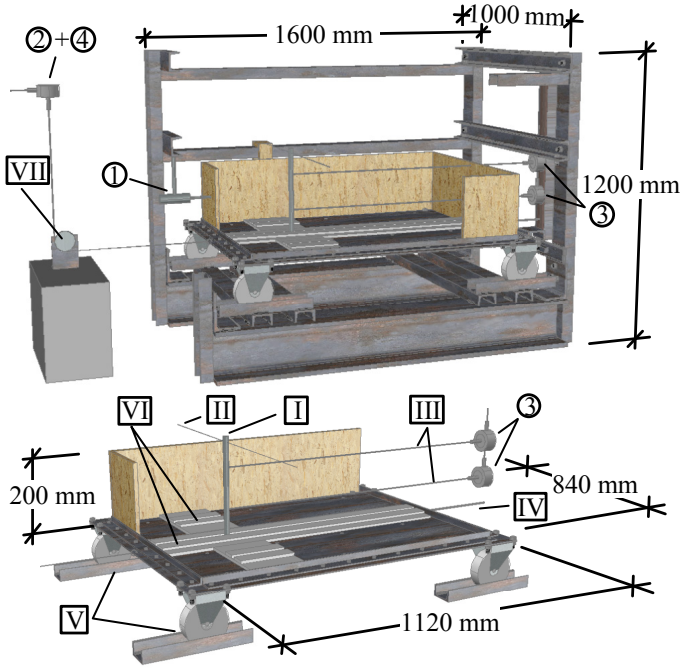

① 2 displacement transducers. ②+④ displacement transducer and load cell for hydraulic press. ③ load cells for model pile. I Model pile. II Temporary guying for the model pile during sample preparation. III Guyings between model pile and load cells. IV Spring. V Polyamid wheels guided in steel channel sections. VI Adjustable guide rail at the pile base. VII Ginny wheel between cart and hydraulic press.

Figure 3. Test set up.

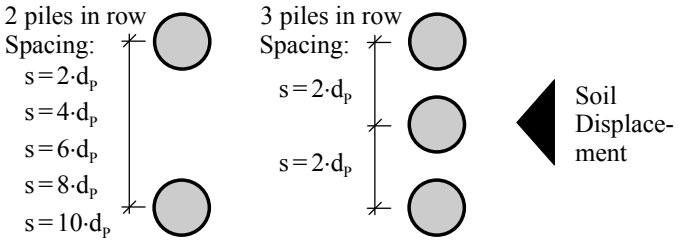

Figure 4. Pile row configurations in the model tests.

During two tests, the pore pressure at the pile shaft was measured by means of pipes (Inner diameter/Outer diameter: 0.5 mm/1.5 mm) protected by a geotextile filter to prevent the infiltration of soil particles. The water-filled pipes were connected to external pore-pressure cells. To minimize the influence of the pipes on pile-soil-interaction, the pipes were placed in grooves and only model piles with the maximum diameter of d_p = 40 mm were employed.

All tests except the single piles with pore pressure measurement were analyzed with the PIV-Method (e. g. White & Take 2002). Preliminary tests showed that by dispersing fine sand as a tracer on top of the Kaolin clay surface, the measurement deviations ranged in the same order of magnitude as for tests on sand only, i. e. 2 % to 3 % related to the displacement of the box.

The digital reflex camera operated so that images were obtained every 1 mm of soil displacement. The field of view corresponded to an object space pixel size of approximately 0.25 mm.

Table 3. Model test configurations.

Test	w (%)	s_u (kPa)	d_p or a_p (mm)	v (mm/min)
Single piles				
T01/T11	39.5/39.4	2.4/2.4	20	0.1
T02/T10	39.6/39.9	2.3/2.2	40	0.1
T03/T06	39.4/39.4	2.4/2.4	30	0.1
T04/T08	39.2/40.2	2.5/2.1	30	1
T05/T09	39.0/39.6	2.6/2.3	30**	0.1
T07/T17	38.5/46.2	2.7/0.8	30/40	0.01
T12	34.5	5.2	30	0.1
T13/T15	44.5/48.0	1.1/0.6	40	1
T14/T16	46.7/47.1	0.8/0.7	40	0.1
T18/T19	46.7/45.7	0.8/0.9	30/20	0.1
T20/T23	38.5/39.3	2.7/2.4	20**/40**	0.1
T21*/T22*	46.0/39.1	0.9/2.5	30	0.1
Single piles with pore pressure measurements				
T1P/T2P	47.1/48.0	0.7/0.6	40	1
Pile rows				
T2d/T4d	39.3/39.2	2.4/2.4	20	0.1
T6d/T8d	39.3/39.9	2.4/2.2	20	0.1
T10d	39.5	2.4	20	0.1
T2d3_1/2	38.6/39.5	2.7/2.4	20	0.1

w = water content; s_u = undrained shear strength; d_p = pile diameter; a_p = pile edge length; v = velocity of the soil body

* rough pile; ** square pile

3.2 *Soil properties and sample preparation*

Kaolin clay (Table 4) with a very soft consistency and water contents close to the liquid limit or even higher yielding a liquidity index $I_L \geq 1$ was placed in approximately 3 cm thick layers in the box. Every layer was smoothened before the next layer was placed. Under the assumption that the structure of Kaolin clay does not change significantly during consolidation (Soumaya 2005) and to proceed with the testing program in a reasonable time frame, the tests started immediately after the soil placement, i. e. no time was given for consolidation under self-weight. Figure 5 shows the variation of the undrained shear strength s_u with water content w. The undrained shear strength was determined in the test box in preliminary tests and after the actual tests with a small vane penetrometer.

3.3 *Test results*

In the scope of this paper, the lateral pressure acting on the pile p and the relative displacement between the pile and the soil body δ were normalized by the undrained shear strength s_u and the pile diameter d_p or pile edge length a_p, respectively. The lateral pressure of the pile p was derived from the measured forces on the pile divided by the pile length and the pile diameter or pile edge length, respectively. The relative displacement between pile and soil body δ was assumed to be equivalent to the displacement of the box.

Table 4. Kaolin clay properties.

Grain density ρ_s	g/cm³	2.71
Dry density ρ_d	g/cm³	1.24
Atterberg limits LL; PL	%	36.4; 18.6
Angle of internal friction ϕ' (critical state)		20°
Slope of the compression line λ	-	0.114
Slope of the swelling line κ	-	0.044
Permeability k	m/s	$2 \cdot 10^{-9}$ to $8 \cdot 10^{-10}$

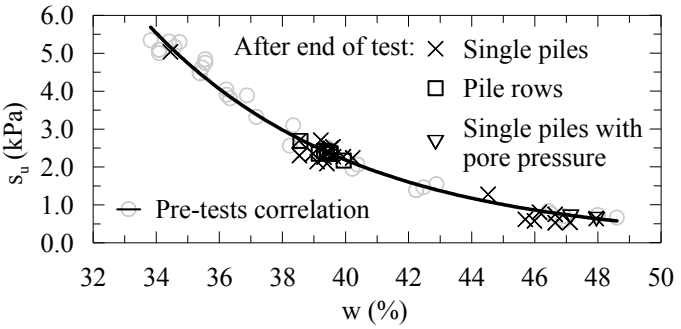

Figure 5. Variation of undrained shear strength s_u with water content w.

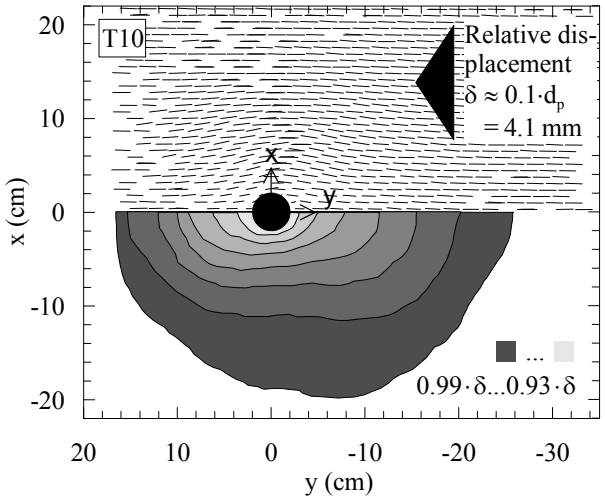

Figure 6. PIV analysis of test T10: Vector plot (top) and contour lines of (bottom) of relative displacement.

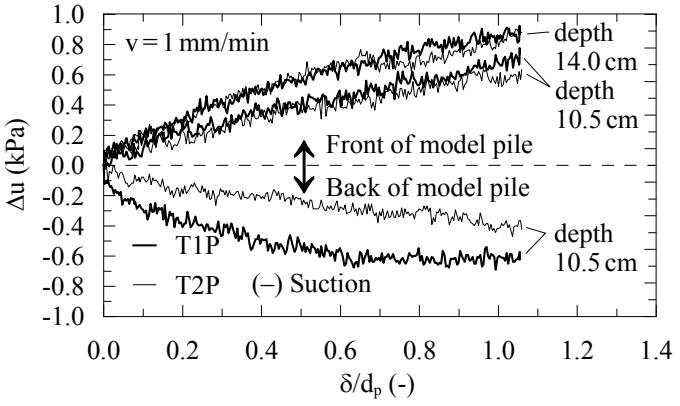

Figure 7. Variation of excess pore pressure Δu with normalized soil displacement δ/d_p.

As an example, Figure 6 shows the result of the PIV-analysis of test T10 for a relative displacement between pile and soil, i. e. the displacement of the box, of $\delta \approx 0.1 \cdot d_p \approx 4$ mm. The flow of the soil around the pile was recognizable up to relative displacements of $\delta \approx 1.0 \cdot d_p$. The soil at the back of the pile separated from the pile shaft and holes of various area sizes and depths developed.

The pore pressure measurements exhibited an increase of the pore pressure at the front of the pile ($\Delta u > 0$) during the test with the pore pressures at a depth of 14.0 cm higher than at a depth of 10.5 cm (Figure 7). At the back of the pile the pore pressures decreased ($\Delta u < 0$). In part, this might be the result of suction stresses developing during the test. On the other hand, the holes at the pile shaft with depths of up to 10 cm might influence the pore pressure measurements at the pile back. However, the effect of the holes on the pore pressure could not be specified in detail, so far.

Figure 8 and Figure 9 show the variation of normalized soil displacement δ/d_p with the normalized pressure acting on the piles p/s_u for smooth circular and square piles. The displacement rate of the soil body was held constant at v = 0.1 mm/min in these tests. The tests with circular piles (Figure 8) exhibit increased values for p/s_u for higher water contents w, which correlate with low values of s_u (Figure 5). However, this might be caused by difficulties in establishing rather low values of s_u with the vane penetrometer.

In accordance with Equation 1, there appears to be no significant influence of d_p or a_p, respectively, and s_u, at least for approximately $w \leq 40$ % ($s_u \geq 2$ kPa), on the normalized pressure acting on the piles (Equation 2).

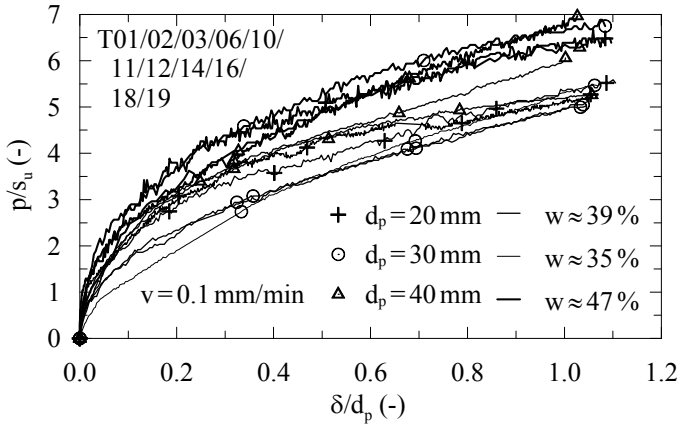

Figure 8. Circular piles: Variation of the normalized pressure acting on the piles p/s_u with normalized soil displacement δ/d_p.

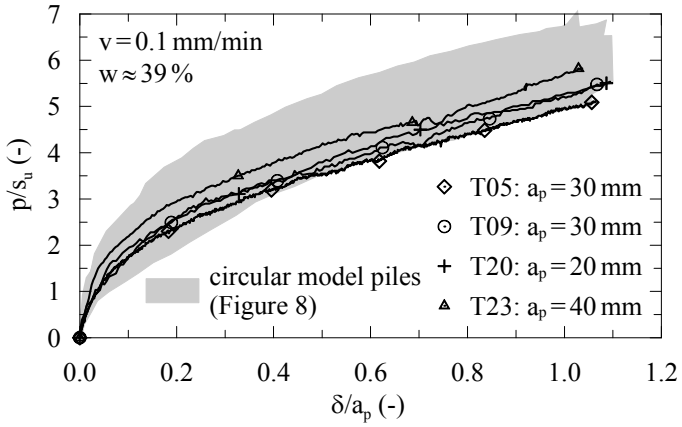

Figure 9. Square piles: Variation of the normalized pressure acting on the piles p/s_u with normalized soil displacement δ/a_p.

$$\frac{p}{d_p} = \frac{P_u}{d_p \cdot s_u} \approx \text{const. or } \frac{p}{a_p} = \frac{P_u}{a_p \cdot s_u} \approx \text{const.} \qquad (2)$$

However, as the normalized pressures are still increasing it suggests that the maximum values may be higher than those stated.

Due to the larger shaft area and the resulting higher shaft resistance, one would expect increased lateral pressure for square piles with edge length a_p compared to circular piles with $d_p = a_p$. However, this could not be observed in the model tests (Figure 9). The square piles lay within the bandwidth of results for the circular piles.

Figure 10 shows a comparison of test results for smooth piles (T03, T06 & T18) and rough piles (T22 & T21) for water contents of $w \approx 39$ % and $w \approx 47$ %. The rough piles exhibit higher lateral pressures than the smooth piles. Moreover, it appears that the difference between smooth and rough piles is more pronounced for higher values of s_u.

Figure 11 investigates the influence of the displacement rate of the soil v for $w \approx 39$ % and $w \approx 47$ %. An increase of the displacement rate of $v = 0.1$ mm/min to $v = 1$ mm/min yields an increase of the lateral pressure of 15 % to 25 %. However, based on the work of Gudehus & Leinenkugel (1978) an increase of the lateral pressure of 5 % would have been expected for an increase of the displacement rate of 10 %. To clarify if the effect observed in the current model tests is related solely to the viscosity of the soil or if an increase of excess pore pressures with increasing displacement rate makes a contribution, too, further investigations are necessary.

As an example for the model test on pile rows, selected results for two piles in a row are presented in the following. Figure 12 compares pile rows with varying pile spacing with single piles for $w \approx 39$ % and $v = 0.1$ mm/min. In contrast to the results published by Wenz (1963) and Matsui et al. (1982), the lateral pressures acting on the piles in the row are smaller than the lateral pressures on a comparable single pile. Similar results as in the current model tests were presented by Pan et al. (2002).

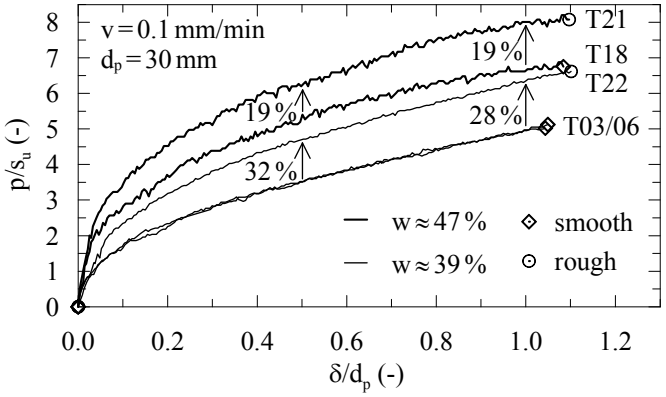

Figure 10. Influence of the pile roughness: Variation of the normalized pressure acting on the piles p/s_u with normalized soil displacement δ/d_p.

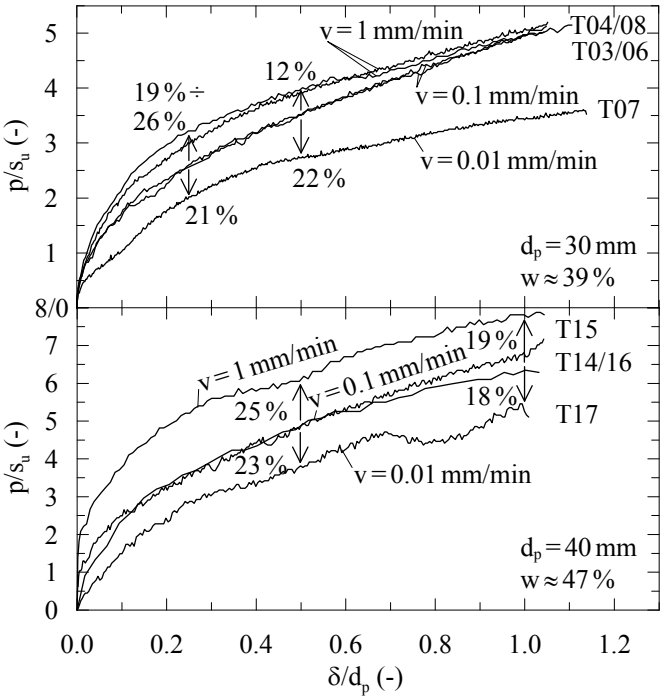

Figure 11. Influence of the displacement rate v: Variation of the normalized pressure acting on the piles p/s_u with normalized soil displacement δ/d_p.

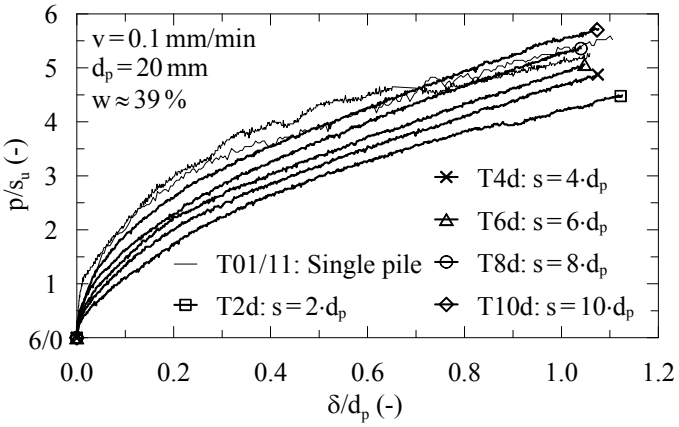

Figure 12. Pile rows: Variation of the normalized pressure acting on the piles p/s_u with normalized soil displacement δ/d_p.

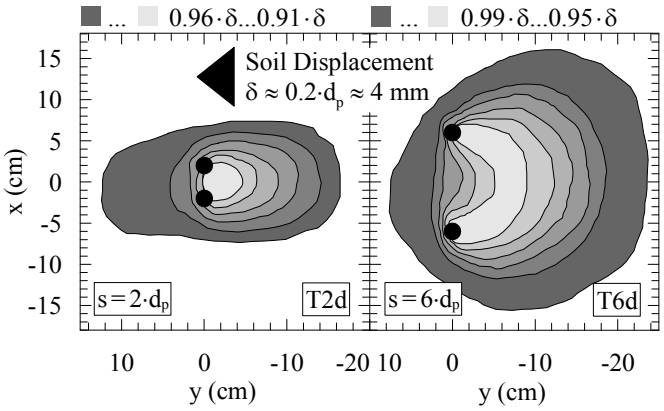

Figure 13. PIV analyses of tests T2d and T6d: Contour lines of soil displacement.

Figure 13 shows the results of the PIV-analyses for rows with a pile spacing of $s = 2 \cdot d_p$ (T2d) and $s = 6 \cdot d_p$ (T6d), respectively, and a relative displacement of $\delta \approx 0.2 \cdot d_p \approx 4$ mm. The PIV-analyses illustrate how the soil movements are constrained by the piles. For $s = 6 \cdot d_p$ an arching effect is visible. A compari-

son of the areas influenced by the piles shows an increase of approximately 220 % (T2d) to 260 % (T6d) compared to a single pile. However, this observation appears to be in conflict with the lateral pressure acting on the group piles being smaller than the lateral pressure acting on a single pile (Figure 12).

4 CONCLUSIONS

The model test on single piles confirmed the significant influence of the pile roughness and of the displacement rate of the soil on the lateral pressure acting on the piles while an influence of the pile shape could not be observed. For a final assessment of the influence of the displacement rate, the excess pore pressures acting at the pile front and the suction stresses acting at the pile back, respectively, as measured in the current tests needs to be further investigated.

For the maximum applied normalized relative displacement $\delta/d_p \approx 1$, the model tests on single piles yield maximum normalized lateral pressures in a range between $p/s_u \approx 3.5$ and $p/s_u \approx 8$, which lie within the bandwidth of values documented in the literature (Table 2) for $P_u/(d_p \cdot s_u)$ or $P_u/(a_p \cdot s_u)$, respectively. However, since the lateral pressure is increasing with increasing normalized relative displacement δ/d_p or δ/a_p, respectively, these values should not be considered as ultimate values. Another factor contributing to the relatively small observed p/su-values compared to theoretical solutions based on deep planar flow mechanisms (e. g. Randolph & Houlsby 1984) might be that shallow wedge shaped failure mechanisms, as observed for example by Knappett et al. (2010), developed in the presented tests.

For pile rows comprising two piles up to a spacing of $s = 8 \cdot d_p$, smaller lateral pressures were measured than for a comparable single pile. This result needs further investigation including numerical analysis to study group behaviour. The PIV-analyses carried out, indicates arching effects between piles which can result in increased lateral pressures.

In the next phase of the research project the results of the model tests will be applied for the verification of a numerical model. With the numerical model parametric studies will be carried out, to improve available design approaches.

REFERENCES

Bransby M. F. 1995. Piled Foundations adjacent to surcharge Loads. PhD thesis, University of Cambridge, UK.

Brinch Hansen, J. & Lundgren, H. 1960. Hauptprobleme der Bodenmechanik. Springer-Verlag. Berlin: pp. 266–268.

Chen, L. T. 1994. The effect of lateral soil movements on pile foundation. PhD thesis, University of Sydney, Australia.

De Beer, E. E. 1977. The effects of horizontal loads on piles, due to surcharge or seismic effects. *Proc. IX ICSMFE, Speciality Session, Vol. 10,* Tokyo: pp. 547–558.

Deutsche Gesellschaft für Geotechnik (DGGT), AK 2.1 2012. Empfehlungen des Arbeitskreises Pfähle – EA Pfähle. 2nd Edition, Ernst & Sohn.

Gudehus, G. & Leinenkugel, H-J. 1978. Fließdruck und Fließbewegung in bindigen Boden: Neue Methoden. *Baugrundtagung,* Essen: pp. 411–429.

Jeong, S. & Seo, D. & Lee, J. & Park, J. 2004. Time-dependent behavior of pile groups by staged construction of an adjacent embankment on soft clay. *Canadian Geotechnical Journal, Vol. 41, Issue 4:* pp. 644–656.

Knappett, J. A., Mohammadi, S. & Griffin, C. 2010. Lateral spreading forces on bridge piers and pile caps in laterally spreading soil: effect of angle of incidence. *Journal of Geotechnical and Geoenvironmental Engineering, Vol. 136, Issue 12:* pp. 1589–1599.

Matsui, T. & Hong, W. P. & Ito, T. 1982. Earth pressures on piles in a row due to lateral soil movements. *Soils and Foundations, Vol. 22, Issue 2:* pp. 71–81.

Ong, D. E. L. & Leung, C. F. & Chow, Y. K. 2003. Time-dependent pile behavior due to excavation-induced soil movement in clay. *Proc. XII PCSMGE. MIT, USA, Vol. 2:* pp. 2035–2040.

Pan, J. L. & Goh, A. T. C. & Wong, K. S. & Teh, D. I. 2000. Model tests on single piles in soft clay. *Canadian Geotechnical Journal, Vol. 37:* pp. 890–897.

Pan, J. L. & Goh, A. T. C. & Wong, K. S. & Teh, D. I. 2002. Ultimate soil pressures for piles subjected to lateral soil movements. *Journal of Geotechnical and Geoenvironmental Engineering, Vol. 128, Issue 6:* pp. 530–535.

Randolph, M. F. & Houlsby, G. T. 1984. The limiting pressure on a circular pile loaded laterally in cohesive soil. *Géotechnique, Vol. 34, Issue 4:* pp. 613–623.

Schenk, W. & Smoltczyk, H-U. 1966. Pfahlroste, Berechnung und Ausbildung. *Grundbau-Taschenbuch, Abschnitt 2.7, Band 1, 2. Auflage, Ernst & Sohn, Berlin:* pp. 658–715.

Soumaya, 2005. Setzungsverhalten von Flachgründungen in normalkonsolidierten bindigen Böden. *Schriftenreihe Geotechnik der Universität Kassel*, Heft 16.

Springman, S. M. 1989. Lateral Loading on Piles Due to Simulated Embankment Construction. PhD thesis, University of Cambridge, UK.

Stewart, D. P. 1992. Lateral loading of piled bridge abutments due to embankment construction. PhD thesis, University of Western Australia, Australia.

Stewart, D. P. & Jewell, J. R. & Randolph, M. F. 1994. Design of piled bridge abutments on soft clay for loading from lateral soil movements. *Geotechnique, 42 (2):* pp. 277–296.

Wenz, K.-P. 1963. Über die Größe des Seitendrucks auf Pfähle in bindigen Erdstoffen, Institut für Boden- und Felsmechanik der Universität Karlsruhe, Issue 12.

Wenz, K.-P. 1972. Seitendruck auf Pfähle in weichen bindigen Erdstoffen, *Baugrundtagung:* pp. 681–690.

White, D. J. & Take, W. A. 2002: GeoPIV: particle image velocimetry (PIV) software for use in geotechnical testing. Technical Report, Cambridge University Department of Engineering, Cambridge, UK.

PROCEEDINGS OF THE 8TH INTERNATIONAL CONFERENCE ON PHYSICAL MODELLING IN GEOTECHNICS 2014 (ICPMG 2014), PERTH, AUSTRALIA, 14–17 JANUARY 2014

Physical Modelling in Geotechnics

Editors

Christophe Gaudin & David White

Centre for Offshore Foundation Systems, The University of Western Australia, Perth, Australia

VOLUME 2

CRC Press

Taylor & Francis Group

Boca Raton London New York Leiden

CRC Press is an imprint of the Taylor & Francis Group, an **informa** business

A BALKEMA BOOK